

CONFIDENTIAL

Copy 6
RM H55A11

NACA RM H55A11

NACA

RESEARCH MEMORANDUM

WING-LOAD MEASUREMENTS OF THE BELL X-5 RESEARCH
AIRPLANE AT A SWEEP ANGLE OF 58.7°

By Richard D. Banner, Robert D. Reed,
and William L. Marcy

High-Speed Flight Station
Edwards, Calif.

CLASSIFICATION CANCELLED

Activity *Naca Res 66* Date *2/2/56*

KN 97

By *inst 2/27/56* See

CLASSIFIED DOCUMENT

This material contains information affecting the National Defense of the United States within the meaning of the espionage laws, Title 18, U.S.C., Secs. 793 and 794, the transmission or revelation of which in any manner to an unauthorized person is prohibited by law.

NATIONAL ADVISORY COMMITTEE FOR AERONAUTICS

WASHINGTON

April 4, 1955

CONFIDENTIAL

NATIONAL ADVISORY COMMITTEE FOR AERONAUTICS

RESEARCH MEMORANDUM

WING-LOAD MEASUREMENTS OF THE BELL X-5 RESEARCH

AIRPLANE AT A SWEEP ANGLE OF 58.7°

By Richard D. Banner, Robert D. Reed,
and William L. Marcy

SUMMARY

A flight investigation has been made over an altitude and lift range to determine the wing loads of the Bell X-5 research airplane at a sweep angle of 58.7° at subsonic and transonic Mach numbers.

The wing loads were nonlinear over the angle-of-attack range from zero to maximum wing lift. The nonlinear trends were more pronounced at angles of attack above the "pitch-up" where there is a reduction in the wing lift and an inboard and forward movement in the center of load.

No apparent effects of altitude on the wing loads were evident from the data obtained in these tests.

INTRODUCTION

As part of the cooperative Air Force--Navy--NACA transonic flight research program, the National Advisory Committee for Aeronautics is utilizing the Bell X-5 variable-sweep research airplane for flight investigations at the NACA High-Speed Flight Station at Edwards, Calif. These flight investigations are aimed at determining loads, the stability and control characteristics, lift and drag, and buffeting characteristics of the airplane at selected sweep angles. Because of the interest in the loads and stability characteristics at high sweep angles, the first complete investigation on this airplane was made at a sweep angle of 58.7° which was the maximum sweep obtainable. The wing-loads measurements at this sweep angle are presented herein. Preliminary results of the tail-load measurements at several sweep angles during the demonstration tests are presented in reference 1.

SYMBOLS

BM_W	wing-panel bending moment about the gage station, ft-lb
$b_W/2$	span of left wing panel outboard of gage station, ft
C_{B_W}	wing-panel bending-moment coefficient, $\frac{BM_W}{q \frac{S_W}{2} \frac{b_W}{2}}$
C_m $\bar{c}_W/4$	wing-panel pitching-moment coefficient about the quarter chord of the M.A.C. _W , $\frac{M_W}{q \frac{S_W}{2} \bar{c}_W}$
C_N	normal-force coefficient
C_{N_A}	airplane normal-force coefficient, nW/qS
C_{N_W}	wing-panel normal-force coefficient, $\frac{L_W}{q \frac{S_W}{2}}$
c	chord at any section along span, ft
c_W	streamwise chord at any section along wing-panel span, ft
\bar{c}_W , M.A.C. _W	mean aerodynamic chord of wing panel, $\frac{\int_0^{b_W/2} c_W^2 dy}{\int_0^{b_W/2} c_W dy}$
g	acceleration due to gravity, ft/sec ²
h_p	pressure altitude, ft
L_W	aerodynamic wing-panel load, lb
M	Mach number
M_W	wing-panel pitching moment, ft-lb
n	airplane normal acceleration, g units

q	dynamic pressure, $\rho V^2/2$, lb/sq ft
S	area of wing bounded by leading edge and trailing edge extended to the airplane line of symmetry disregarding fillets, sq ft
$S_W/2$	wing-panel area outboard of left wing gage station, sq ft
V	free-stream velocity, ft/sec
W	airplane gross weight, lb
x_{cp}	wing-panel chordwise center of pressure, percent \bar{c}_W
y_{cp}	wing-panel spanwise center of pressure, percent $b_W/2$
y	lateral displacement, ft
α_i	indicated airplane angle of attack, deg
ρ	mass density of air, slugs/ft ³

Subscript:

max maximum

AIRPLANE

The Bell X-5 research airplane incorporates a wing which is variable in flight from a sweep angle of about 20° to about 58.7°. It is a single-place airplane powered by an Allison J35-A-17 jet engine. A photograph of the airplane in the 58.7° sweep configuration utilized in this investigation is shown in figure 1 and a three-view drawing of the airplane is shown in figure 2.

The airplane physical characteristics in the 58.7° sweepback configuration are given in table I. All distances on the airplane are measured as a distance aft of fuselage station zero as shown on figure 2.

INSTRUMENTATION AND ACCURACY

Standard NACA recording instruments are installed in the airplane to measure the following quantities pertinent to this investigation:

Airspeed
Altitude
Angle of attack and angle of sideslip
Normal, longitudinal, and transverse accelerations
Pitching angular velocity and acceleration
Rolling angular velocity
Yawing angular velocity and acceleration
Control surface positions
Wing sweep angle

Shear, bending moment, and pitching moment on the left wing panel are measured by strain gages installed on the spar and skin at the wing root station 33.9 inches from the airplane center line as shown in figure 2. The outputs of these strain gages are recorded on a multichannel recording oscillograph. Based on the results of a static calibration and an evaluation of the strain-gage responses in flight, the estimated accuracies of the measured shear, bending moment, and pitching moment are ± 100 pounds, ± 400 ft-lb, and ± 200 ft-lb, respectively.

In order to minimize the errors in total pressure measurement an NACA type A-6 total pressure head described in reference 2 was mounted on the nose boom and the static pressure error was determined in flight. The total estimated error in Mach number is within ± 0.01 . The estimated error in the determination of the airplane normal-force coefficient is ± 0.03 . The airplane angle of attack was measured by a vane located on the nose boom and is presented herein as measured data. The estimated accuracy of the angle-of-attack recorder is $\pm 0.5^\circ$.

TESTS

The tests were conducted in the clean configuration with the slats closed and consisted of symmetrical maneuvers through the angle-of-attack range over a Mach number range of 0.61 to 0.97 at an altitude of 40,000 feet, 0.61 to 0.94 at 25,000 feet, and 0.61 to 0.92 at 15,000 feet. The Reynolds number, based on wing mean aerodynamic chord, for these tests varied from 11.5×10^6 to 19.0×10^6 at 40,000 feet and from 38.0×10^6 to 43.0×10^6 at 15,000 feet.

RESULTS AND DISCUSSION

The aerodynamic characteristics of the X-5 wing panel at a sweep angle of 58.7° are presented in figure 3 for representative Mach numbers over the Mach number range from 0.61 to 0.92. Additional data at

M = 0.97 at 40,000 feet are also shown. The data are presented as the variation of Mach number, airplane normal-force coefficient, wing-panel normal-force coefficient, wing-panel bending-moment coefficient, and wing-panel pitching-moment coefficient with angle of attack for test altitudes of 40,000, 25,000, and 15,000 feet.

Over the lift ranges investigated at the three test altitudes the wing-panel lift, bending-moment, and pitching-moment data plotted against angle of attack show no differences in the general shapes of the curves with altitude. Because the small differences in the level of the data generally are within the accuracy of measurement, the above results indicate that there are no apparent effects of altitude on the wing loads. For this reason, subsequent presentation and discussion will be concerned only with the data obtained at an altitude of 40,000 feet where it is possible to describe the wing-panel characteristics over the complete lift range of the airplane.

In figure 3 it can be seen that the wing-panel characteristics and also the airplane normal-force coefficients show nonlinear variations with angle of attack at any one Mach number. This tendency has been reported previously for swept wings. (For example see ref. 3.) If, however, these nonlinear tendencies are considered for all Mach numbers, a definite pattern can be established by which a comparison can be made of the wing-panel characteristics over the Mach number and angle-of-attack range. In the upper portion of figure 4, which is presented as an illustrative example, it can be seen that in traversing the angle-of-attack range the wing panel experiences definite changes in its loading characteristics. These changes may be considered as two regions of linear variation in the wing-panel normal-force, bending-moment, and pitching-moment coefficients with angle of attack; one at low angles of attack, the other at moderate angles of attack. (For convenience these regions will hereinafter be referred to as region A and region B, respectively.) At angles of attack immediately following region B a change in the wing-panel characteristics occurs which coincides approximately with a reduction in the longitudinal stability of the airplane as defined in reference 4. This reduction in airplane stability is associated with a rapid increase in the pitching acceleration which occurs at high lifts during accelerated maneuvers. This region of reduced stability will subsequently be referred to as the "pitch-up" region, and the wing-panel characteristics in this region will be discussed later.

In each of the maneuvers presented in figure 3 vertical lines were placed above the curves to indicate the angles of attack near which a change in wing-panel characteristics occurs. These vertical lines separate the three regions defined above.

The Mach number variation of the three angle-of-attack regions is shown in the lower portion of figure 4. The crosshatched regions

represent the angle-of-attack ranges in which a change in wing-panel characteristics occurs. The curve shown in figure 4 above the pitch-up region is the angle of attack at which the airplane achieved maximum normal-force coefficient and is based on a summary of the flight-test data.

From the data obtained at an altitude of 40,000 feet (fig. 3) a general description of the wing-panel characteristics over the angle-of-attack range at the Mach numbers tested can be summarized as follows:

As the airplane traverses the angle-of-attack region from A to B the wing-panel pitching-moment curve shows an increase in stability and the lift-curve slopes of the airplane and wing panel increase. As the airplane enters the pitch-up region both a stick-fixed and stick-free reduction of stability occur, which is followed by directional instability and aileron overbalance (ref. 4).

As a result the airplane generally develops large sideslip angles following the peak angle of attack. For the lift range of these tests, however, the maximum sideslip angles did not exceed $\pm 2.5^\circ$. It is also near the onset of pitch-up that the wing panel again experiences definite changes in its characteristics. The wing-panel pitching-moment curves indicate an abrupt reduction of wing-panel stability and in most cases unstable tendencies over a very small angle-of-attack range at pitch-up. The wing-panel lift and bending-moment slopes decrease with increasing angle of attack following the pitch-up and continue to decrease up to maximum lift of the airplane. The pitching-moment curve shows stable characteristics again but decreases gradually with increasing angle of attack up to maximum lift. The total airplane lift-curve slope decreases gradually above the pitch-up but does not show the pronounced break in slope at pitch-up as do the wing-panel parameters, indicating that the fuselage contributes a larger percentage of the total airplane lift in the pitch-up region.

Least squares slopes of the airplane and wing-panel normal-force curves of figure 3 were taken in regions A and B as shown in figure 4 and are shown in figure 5 as a variation with Mach number. Considerable data scatter was obtained in an attempt to describe the Mach number variation of the wing-panel and airplane normal-force slopes in both regions; however, some general trends are evident. In region A the wing-panel normal-force-curve slope increases about 30 percent with increasing Mach number in the Mach number range from 0.60 to 0.97. At $M = 0.60$ the value of wing-panel normal-force-curve slope measured about 0.043 per degree. The airplane normal-force-curve slopes show similar trends but the absolute values are approximately 0.004 per degree less than those for the wing panel. At the lower Mach numbers the wing-panel lift-curve slope shows an increase of about 40 percent from region A to region B, whereas the airplane lift-curve slope increases about 37 percent. This

[REDACTED]

difference between the airplane and wing-panel lift-curve slopes between regions A and B decreases with increasing Mach number up to $M = 0.97$ where very small differences in the wing and airplane lift-curve slopes are evident between the two regions.

The theoretical value for the lift-curve slope of the wing panel in the presence of the fuselage at a Mach number of 0.75 was calculated by the method of reference 5 and is shown in figure 5(a). The results indicate good agreement for this case.

Presented in figure 6 are the wing-panel pitching-moment and bending-moment coefficients of figure 3, together with the chordwise and spanwise centers of pressure, plotted as a variation with wing-panel normal-force coefficient. The vertical lines above the curves separate the angle-of-attack regions A, B, and the pitch-up region. The data of this figure show the same characteristic changes in the slopes between regions as was shown in figure 3. These changes are also reflected in the chordwise and spanwise centers of pressure. (Center-of-pressure data are not shown below a wing-panel normal-force coefficient of 0.2 since their locations become meaningless at normal-force coefficients approaching zero.)

As the wing-panel normal-force coefficient increases prior to pitch-up (region A and B) there is a gradual rearward movement of the chordwise center of pressure on the order of about 5 percent of the mean aerodynamic chord of the wing panel associated with only a very slight outboard movement in the spanwise center of pressure at all Mach numbers tested. At pitch-up the wing-panel center-of-load movement abruptly changes direction; the chordwise center of pressure moves forward approximately 5 percent and the spanwise center of pressure moves rapidly inboard 5 to 8 percent of the wing-panel semispan, except near a Mach number of 0.90 where there is essentially no chordwise movement in the center of load at wing-panel normal-force coefficients above the pitch-up.

The most forward position of the center of load is seen to be at about 38 percent of the wing-panel mean aerodynamic chord at a Mach number of 0.61 and a wing-panel normal-force coefficient of 0.255. The most rearward position is at about 50 percent and occurred at a Mach number of 0.74 and a wing-panel normal-force coefficient of about 0.57. The most outboard position of the center of load also occurred at a Mach number of 0.74 and was at about 54 percent of the wing-panel semispan at a wing-panel normal-force coefficient of about 0.40. The furthestmost inboard position was at approximately 43 percent of the wing-panel semispan and occurred at a Mach number of 0.97 and wing-panel normal-force coefficient of about 0.6.

[REDACTED]

The theoretical value for the spanwise center of pressure of the wing panel in the presence of the fuselage at a Mach number of 0.75 was calculated by the method of reference 5 and is presented in figure 6 for comparison with the measured values obtained at Mach numbers of 0.74 and 0.77.

Presented in figure 7 are the wing-panel normal-force, bending-moment, and pitching-moment coefficients for constant airplane normal-force coefficients of 0, 0.2, 0.4, and 0.6. The darkened symbols indicate values which were obtained at normal-force coefficients above the reduction in airplane stability. At constant airplane normal-force coefficients below the reduction in airplane stability the wing-panel normal-force and bending-moment coefficients increase slightly with increasing Mach number and the values of the wing-panel pitching-moment coefficients tend to become more negative. Above the reduction in airplane stability the characteristics of the curves are caused by both the continuous decrease in the wing lift-curve slope and the inboard and forward movement of the center of load as higher lifts above the pitch-up are reached.

CONCLUDING REMARKS

Flight measurements on the Bell X-5 research airplane at a sweep angle of 58.7° have shown that the wing loads exhibit nonlinear trends over the angle-of-attack range from zero to maximum wing lift. These nonlinearities were, in general, more pronounced at angles of attack above the "pitch-up" where there is a reduction in the wing-panel lift-curve slope and an inboard and forward movement in the center of load. These characteristics have been found to exist in the results of wind-tunnel tests of swept wings and emphasize the need of model testing for accurate wing design data when nonlinearities exist.

No apparent effects of altitude on the wing loads were evident over the comparable lift ranges of these tests at altitudes from 40,000 to 15,000 feet.

High-Speed Flight Station,
National Advisory Committee for Aeronautics,
Edwards, Calif., January 5, 1955.

REFERENCES

1. Rogers, John T., and Dunn, Angel H.: Preliminary Results of Horizontal-Tail Load Measurements of the Bell X-5 Research Airplane. NACA RM L52G14, 1952.
2. Gracey, William, Letko, William, and Russell, Walter R.: Wind-Tunnel Investigation of a Number of Total-Pressure Tubes at High Angles of Attack - Subsonic Speeds. NACA TN 2331, 1951. (Supersedes NACA RM L50G19.)
3. Wood, Raymond B., and Fleming, Frank F.: A Transonic-Wing Investigation in the Langley 8-Foot High-Speed Tunnel at High Subsonic Mach Numbers and at a Mach Number of 1.2 - Wing-Fuselage Configuration Having a Wing of 60° Sweepback, Aspect Ratio 4, Taper Ratio 0.6, and NACA 65A006 Airfoil Section. NACA RM L50J25, 1951.
4. Finch, Thomas W., and Walker, Joseph A.: Flight Determination of the Static Longitudinal Stability Boundaries of the Bell X-5 Research Airplane with 59° Sweepback. NACA RM L53A09b, 1953.
5. Zlotnick, Martin, and Diederich, Franklin W.: Theoretical Calculation of the Effect of the Fuselage on the Spanwise Lift Distribution on a Wing. NACA RM L51J19, 1952.

CONFIDENTIAL

TABLE I
PHYSICAL CHARACTERISTICS OF BELL X-5 AIRPLANE
AT A SWEEP ANGLE OF 58.7°

Airplane:	
Weight, lb:	
Full fuel	10,006
Less fuel	7,894
Center-of-gravity position, percent M.A.C.:	
Full fuel	45.0
Less fuel	45.5
Moments of inertia for 58.7° sweep (clean configuration, full fuel), slug-ft ² :	
About X-axis	5,165
About Y-axis	9,495
About Z-axis	10,110
Wing:	
Airfoil section (perpendicular to 38.02-percent-chord line):	
Root	NACA 64(10)A011
Tip	NACA 64(08)A008.28
Sweep angle at 0.25 chord, deg	58.7
Area, sq ft	183.7
Span, ft	20.1
Span between equivalent tips, ft	19.3
Aspect ratio	2.20
Taper ratio	0.411
Mean aerodynamic chord, ft	9.95
Location of leading edge of mean aerodynamic chord, fuselage station	101.2
Incidence root chord, deg	0
Dihedral, deg	0
Geometric twist, deg	0
Wing panel:	
Area, sq ft	113.62
Span, ft	14.33
Mean aerodynamic chord, ft	8.43
Location of leading edge of mean aerodynamic chord, fuselage station	138.6
Horizontal tail:	
Airfoil section (parallel to fuselage center line)	NACA 65A006
Area, sq ft	31.5
Span, ft	9.56
Aspect ratio	2.9
Taper ratio371
Sweep angle at 0.25-percent chord, deg	45
Mean aerodynamic chord, in.	42.8
Vertical tail:	
Airfoil section (parallel to rear fuselage center line)	NACA 65A006
Area, (above aft fuselage center line), sq ft	25.8
Span, perpendicular to aft fuselage center line, ft	6.17
Aspect ratio	1.47
Sweep angle of leading edge, deg	46.6

CONFIDENTIAL



L-87574

Figure 1.- A photograph of the Bell X-5 research airplane.

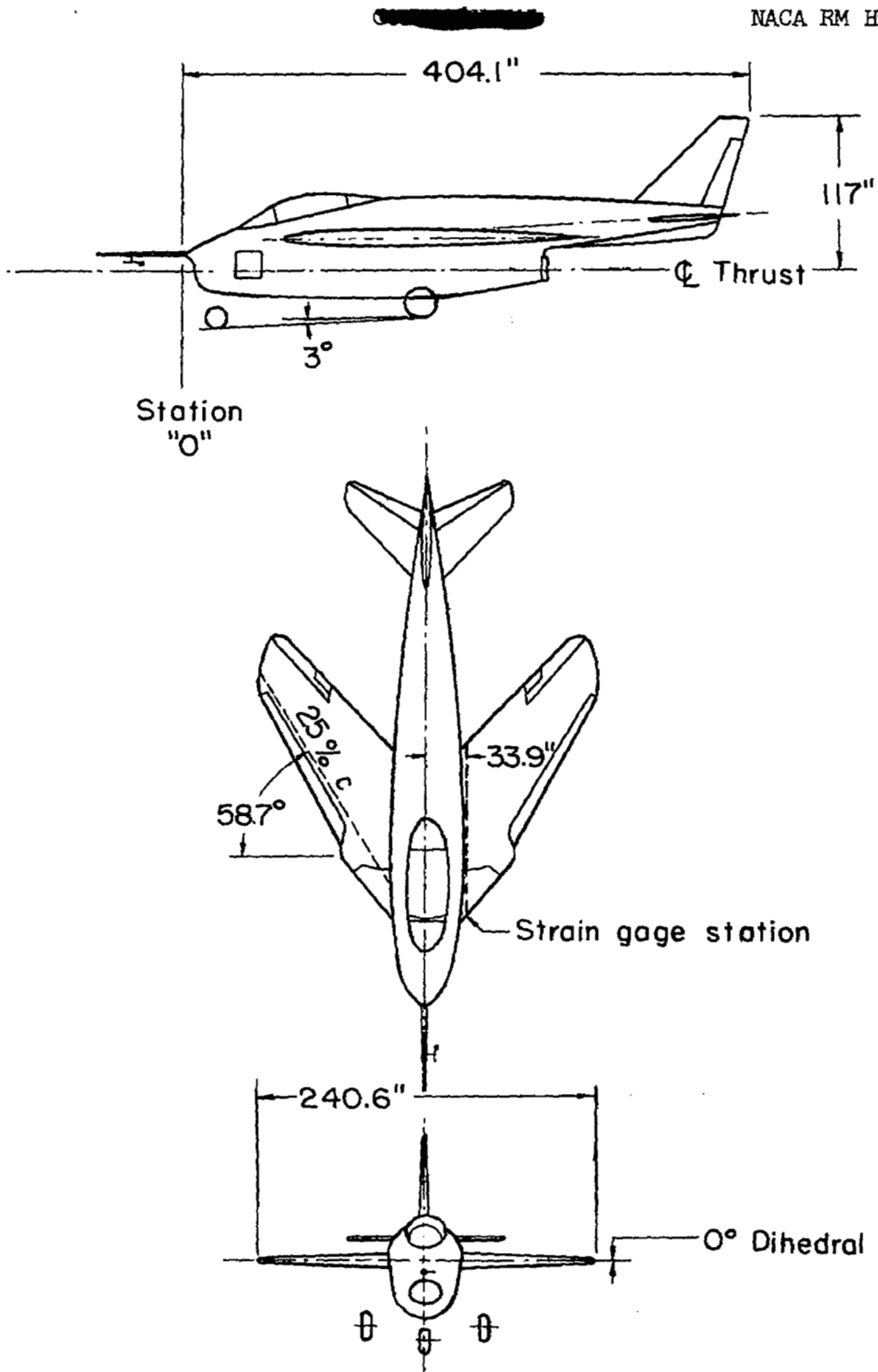
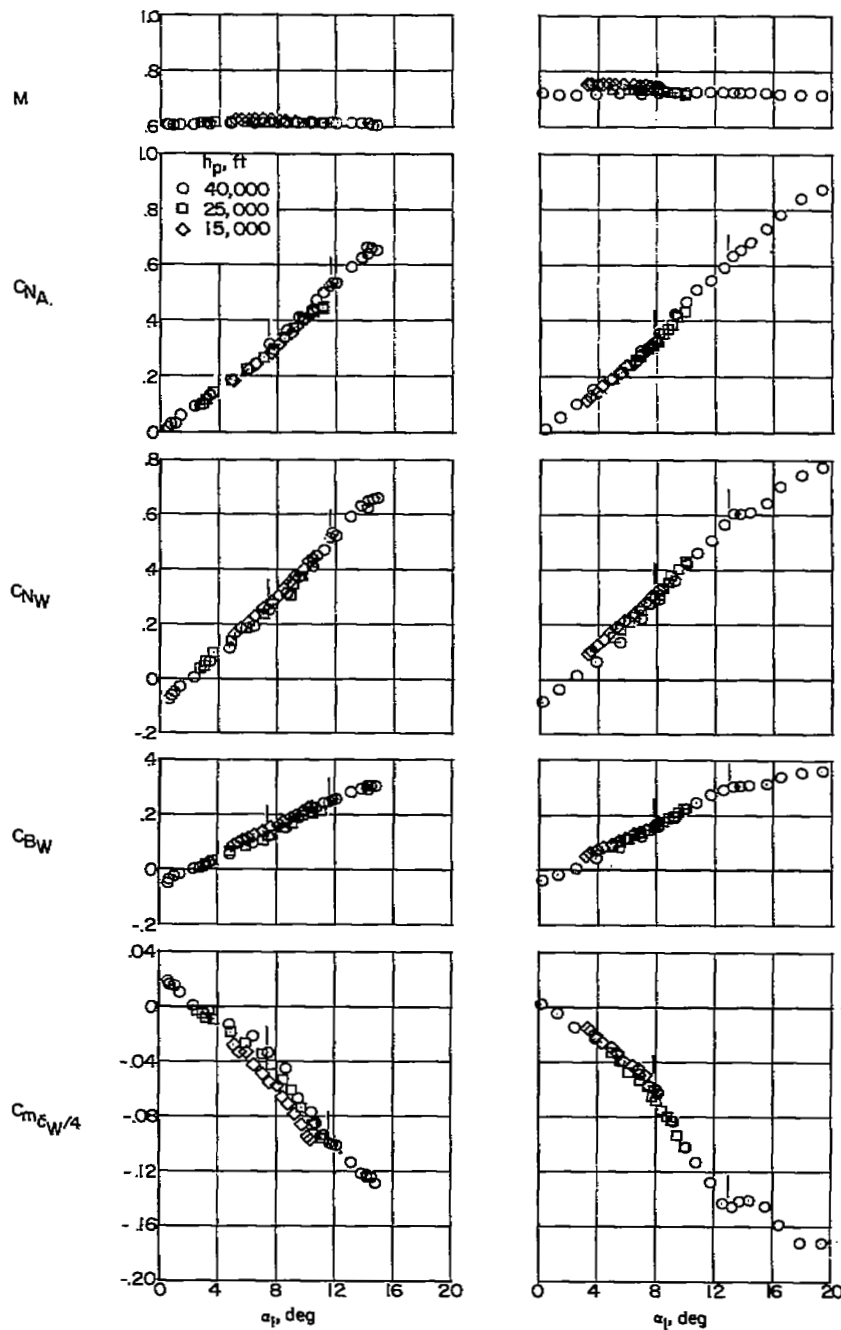


Figure 2.- A three-view drawing of the Bell X-5 research airplane.



(a) $M \approx 0.61$.

(b) $M \approx 0.74$.

Figure 3.- Airplane normal-force and wing-panel characteristics for representative maneuvers over the Mach number range from $M = 0.61$ to $M = 0.97$ at altitudes of 40,000, 25,000, and 15,000 feet.

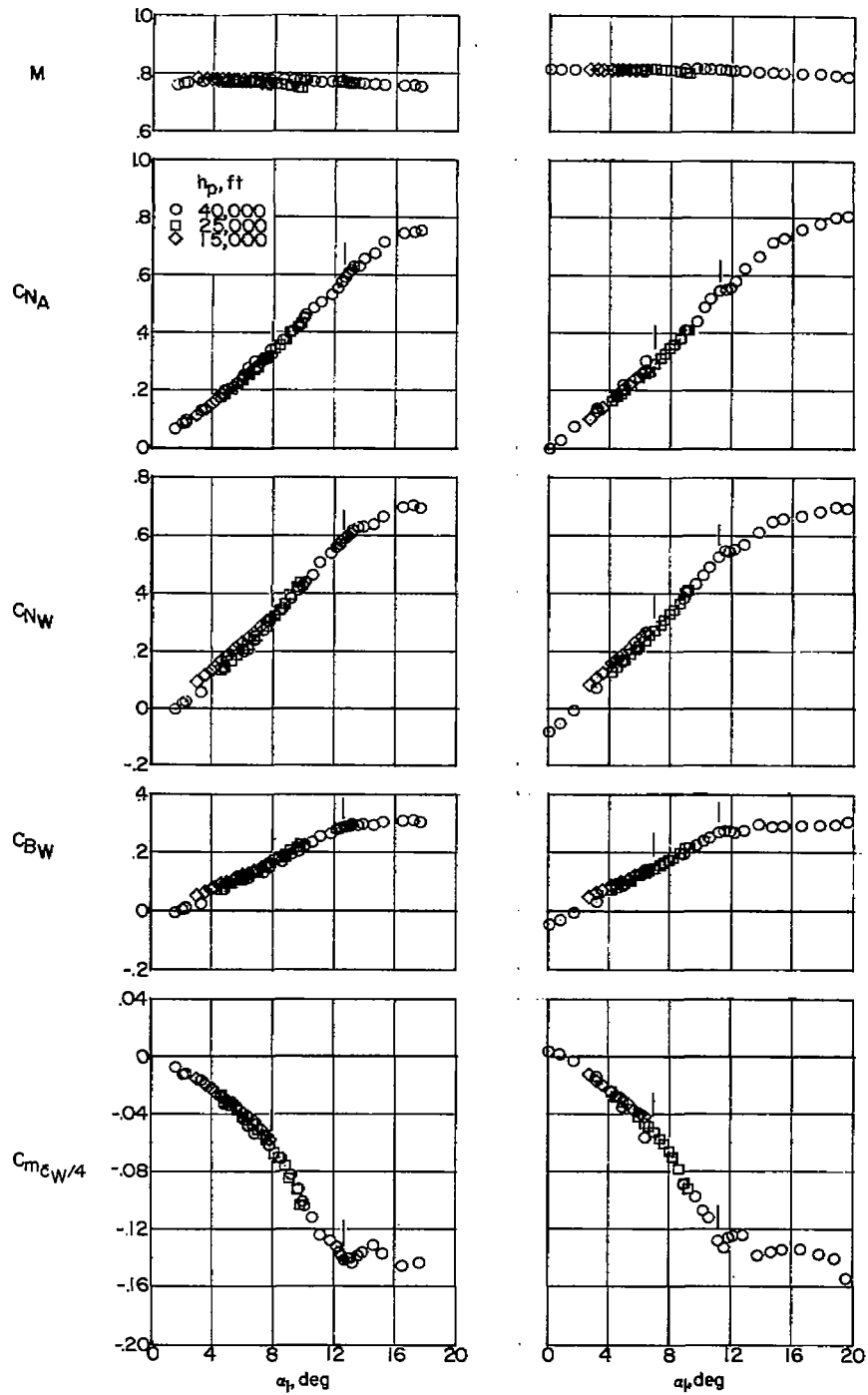
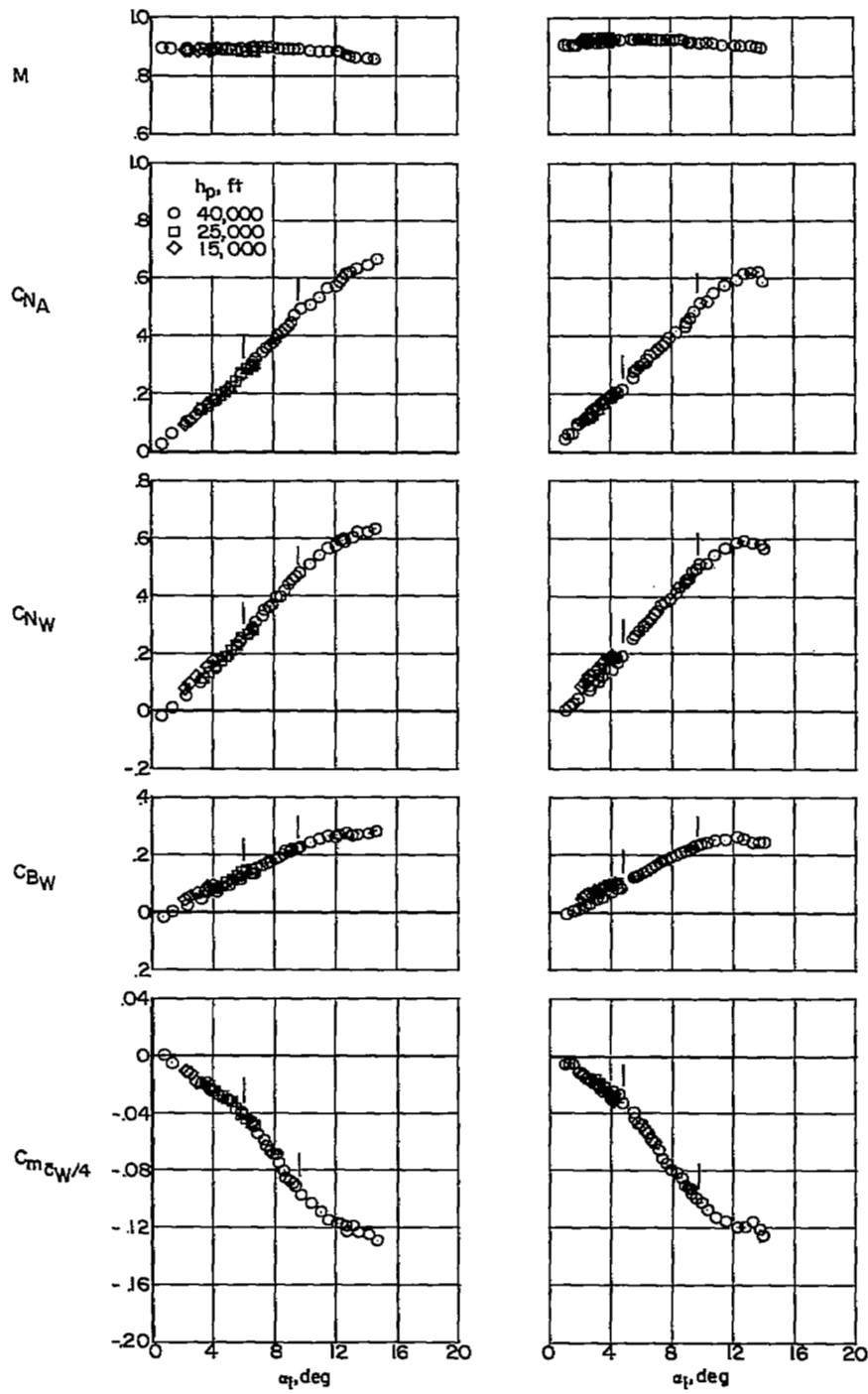
(c) $M \approx 0.77$.(d) $M \approx 0.81$.

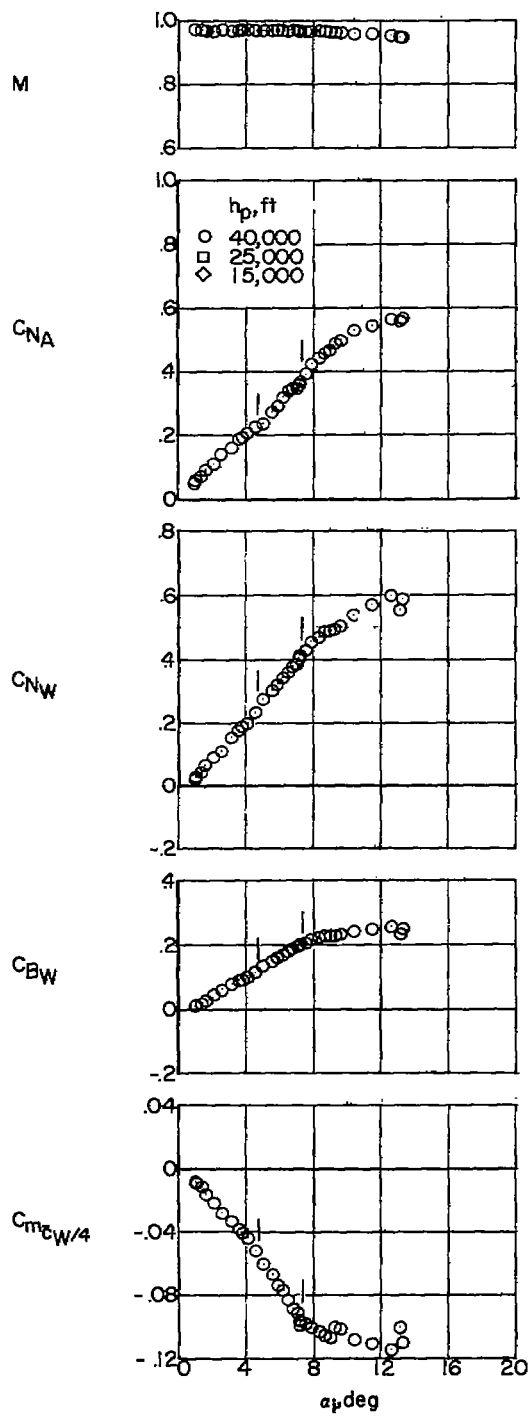
Figure 3.- Continued.



(e) $M \approx 0.89.$

(f) $M \approx 0.92.$

Figure 3.- Continued.



(g) $M \approx 0.97$.

Figure 3.- Concluded.

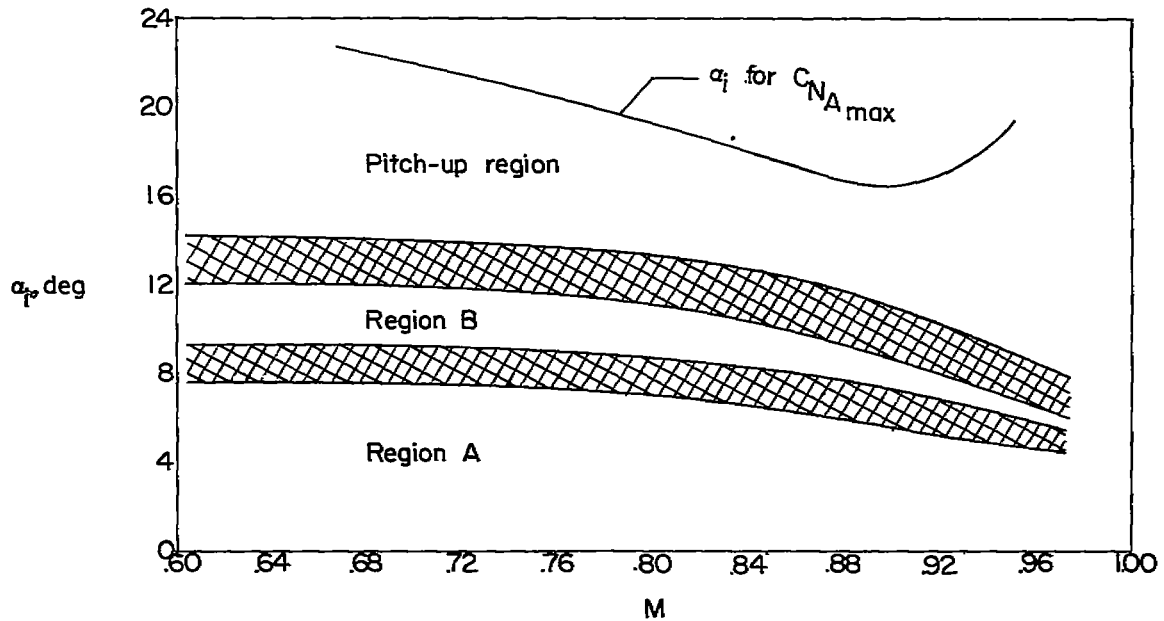
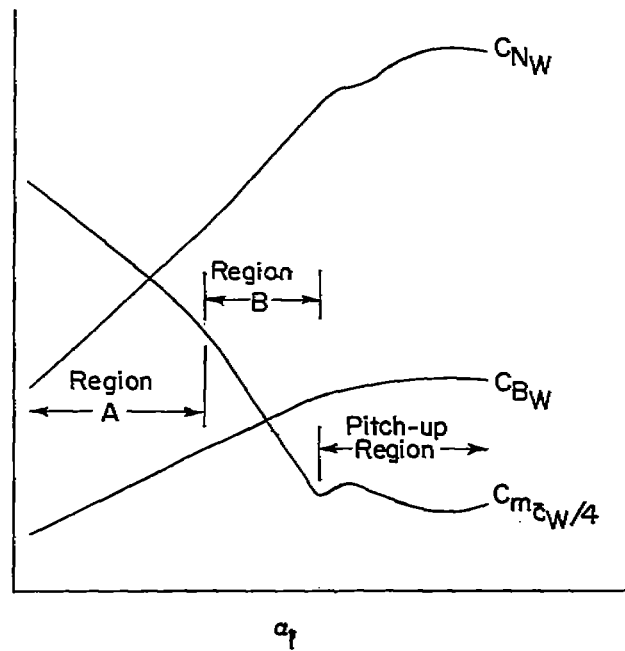
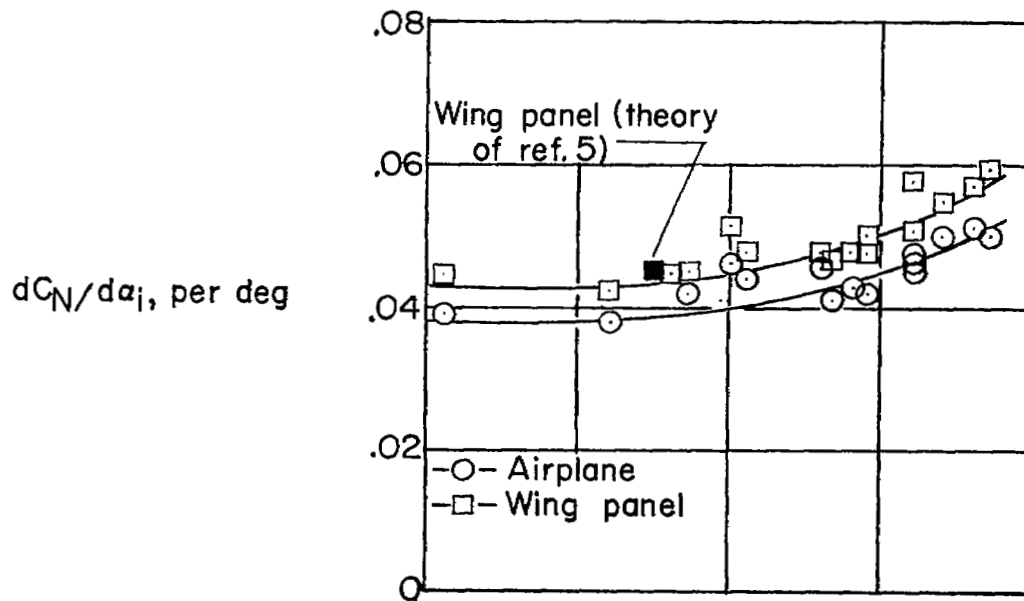
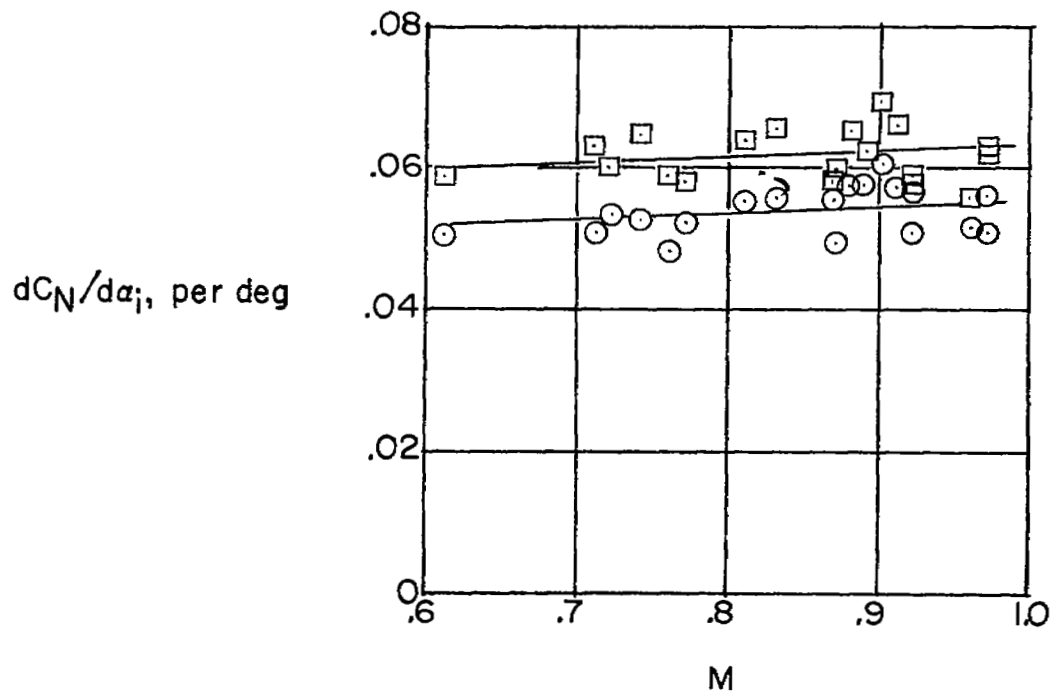


Figure 4.- The Mach number variation of the change in wing-panel characteristics with airplane lift.

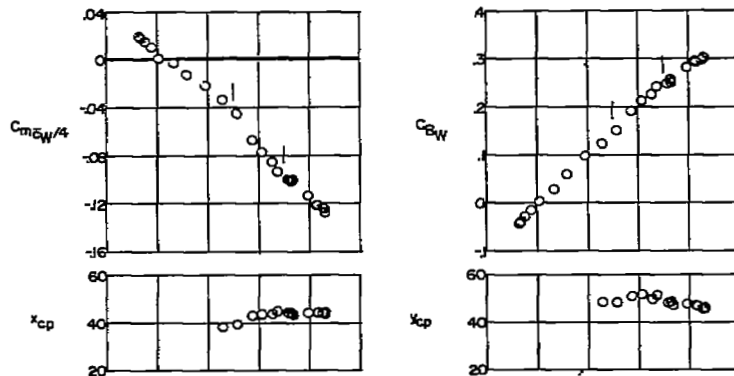


(a) Region A.

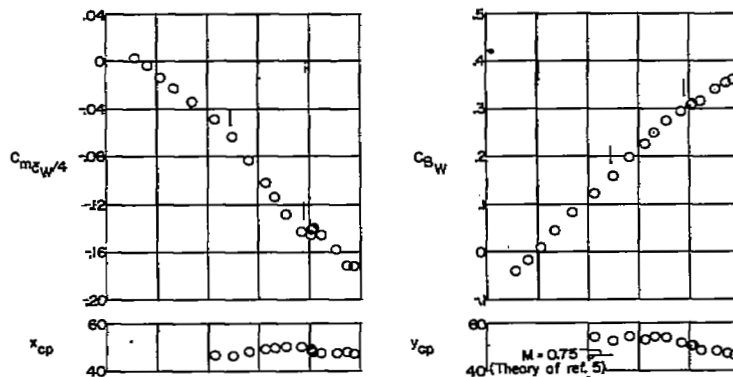


(b) Region B.

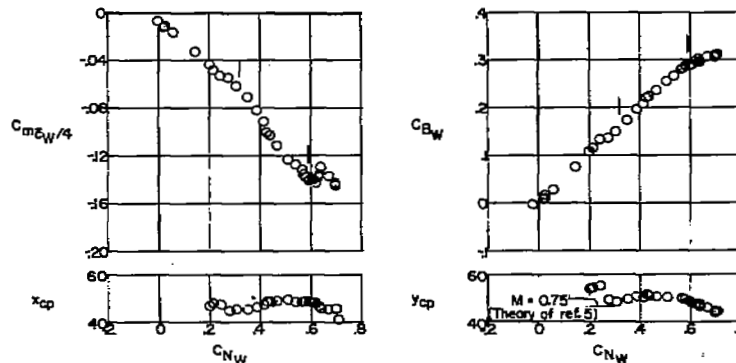
Figure 5.- The Mach number variation of the airplane and wing-panel lift-curve slopes.



(a) $M \approx 0.61$.



(b) $M \approx 0.74$.



(c) $M \approx 0.77$.

Figure 6.- Variations of wing-panel pitching-moment coefficients, bending-moment coefficients, and centers of pressure with wing-panel normal-force coefficient for representative Mach numbers from $M = 0.61$ to $M = 0.97$.

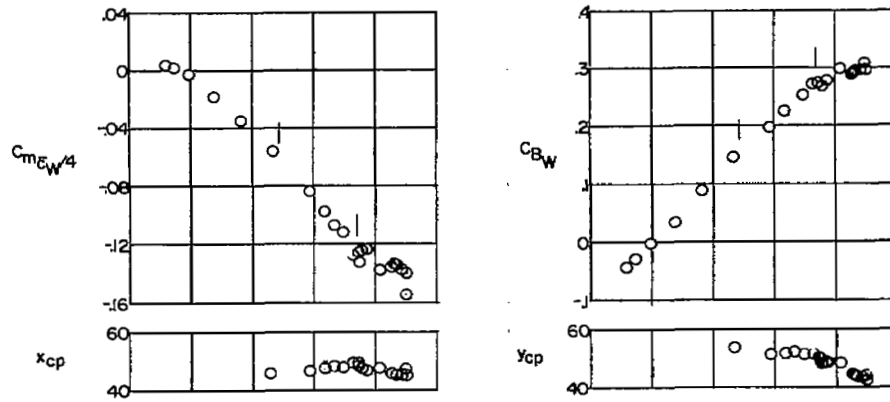
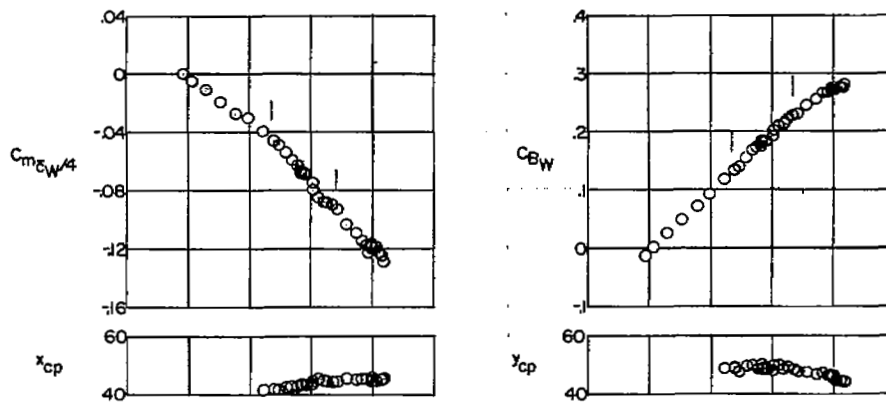
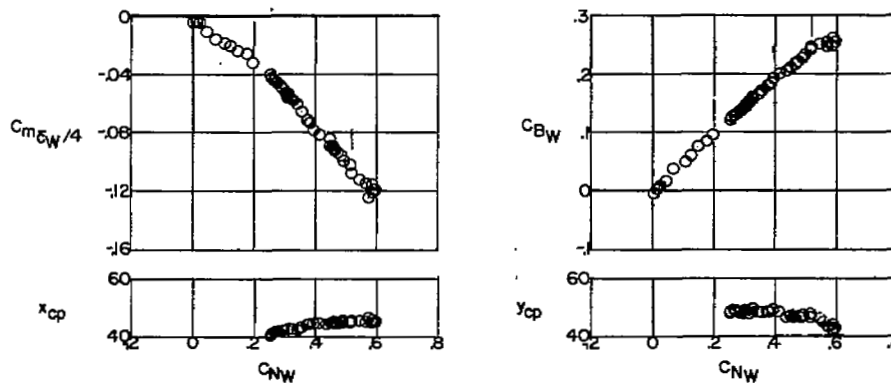
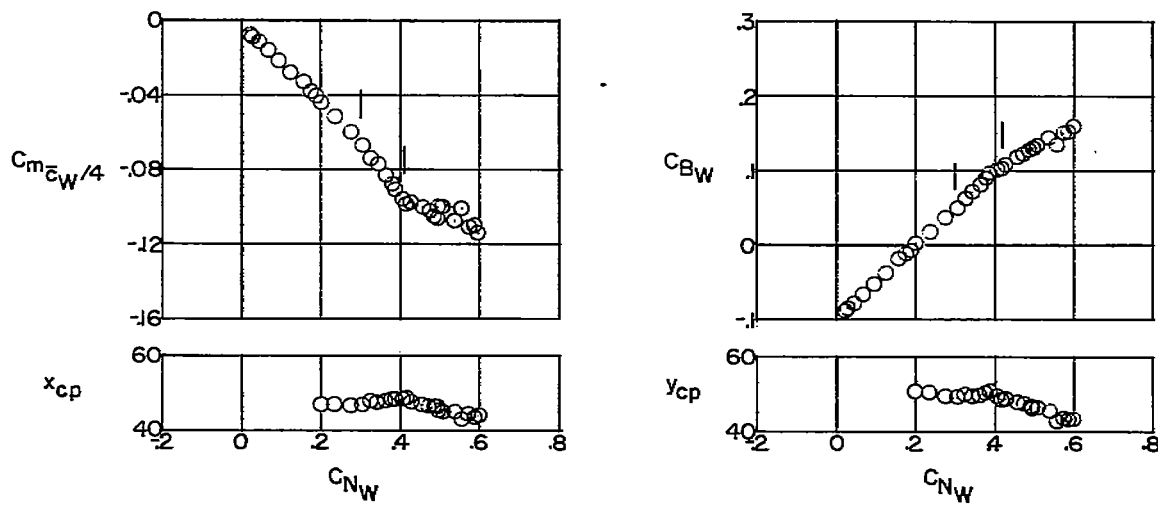
(d) $M \approx 0.81$.(e) $M \approx 0.89$.(f) $M \approx 0.92$.

Figure 6.- Continued.



(g) $M \approx 0.97$.

Figure 6.- Concluded.

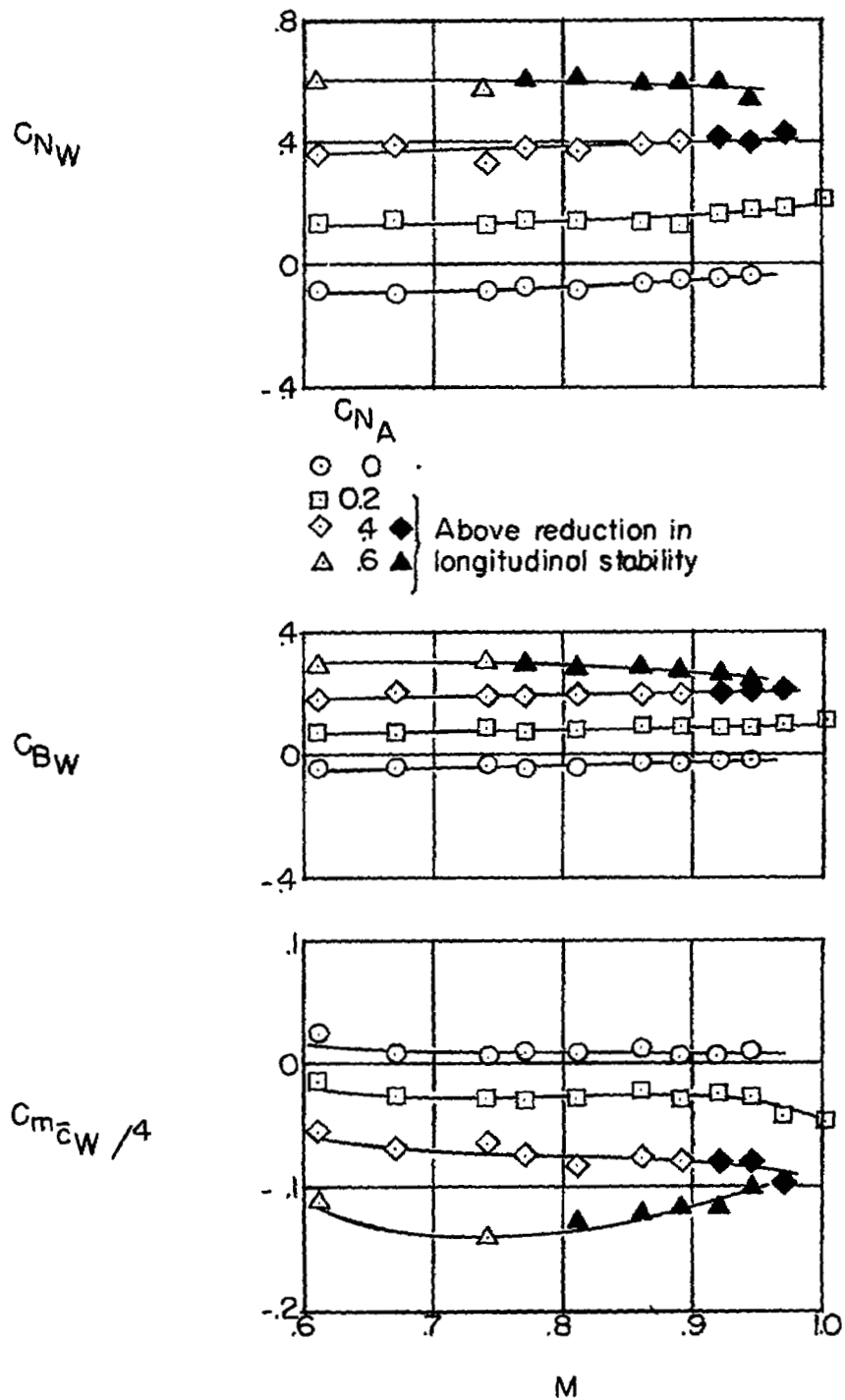


Figure 7.- Mach number variation of the wing-panel characteristics at constant airplane normal-force coefficient.

[REDACTED]



3 1176 01435 9849

[REDACTED]